BRAIN
ORIGINAL ARTICLE

A prefrontal–habenular circuitry regulates social fear behaviour

Yuanyuan Tian,[1,2,†] Junqiang Zheng,[1,3,†] Xiao Zhu,[4,†] Xue Liu,[1] Haoyang Li,[1] Jun Wang,[1,5,6] Qian Yang,[1] Ling-Hui Zeng,[7] Zhiguo Shi,[8] Mengyuan Gong,[4] Yuzheng Hu[4] and Han Xu[1,2,3,5,6]

[†]These authors contributed equally to this work.

The medial prefrontal cortex (mPFC) has been implicated in the pathophysiology of social impairments, including social fear. However, the precise subcortical partners that mediate mPFC dysfunction on social fear behaviour have not been identified.

Using a social fear conditioning paradigm, we induced robust social fear in mice and found that the lateral habenula (LHb) neurons and LHb-projecting mPFC neurons are activated synchronously during social fear expression. Moreover, optogenetic inhibition of the mPFC–LHb projection significantly reduced social fear responses. Importantly, consistent with animal studies, we observed an elevated prefrontal–habenular functional connectivity in subclinical individuals with higher social anxiety characterized by heightened social fear.

These results unravel a crucial role of the prefrontal–habenular circuitry in social fear regulation and suggest that this pathway could serve as a potential target for the treatment of social fear symptoms often observed in many psychiatric disorders.

1 Department of Psychiatry of the Second Affiliated Hospital and School of Brain Science and Brain Medicine, Zhejiang University School of Medicine, Hangzhou 310058, China
2 Nanhu Brain–computer Interface Institute, Hangzhou 311100, China
3 Lingang Laboratory, Shanghai 200031, China
4 Department of Psychology and Behavioral Sciences, Zhejiang University, Hangzhou 310027, China
5 Liangzhu Laboratory, MOE Frontier Science Center for Brain Science and Brain–machine Integration, State Key Laboratory of Brain–machine Intelligence, Zhejiang University, Hangzhou 311121, China
6 NHC and CAMS Key Laboratory of Medical Neurobiology, Zhejiang University, Hangzhou 310058, China
7 Key Laboratory of Novel Targets and Drug Study for Neural Repair of Zhejiang Province, School of Medicine, Hangzhou City University, Hangzhou 310015, China
8 College of Information Science and Electronic Engineering, Zhejiang University, Hangzhou 310027, China

Correspondence to: Han Xu
 Department of Psychiatry of the Second Affiliated Hospital and School of Brain Science and Brain Medicine, Zhejiang University School of Medicine, Hangzhou 310058, China
E-mail: xuhan2014@zju.edu.cn

Correspondence may also be addressed to: Yuzheng Hu
Department of Psychology and Behavioral Sciences, Zhejiang University, Hangzhou 310027, China
E-mail: huyuzheng@zju.edu.cn

Introduction

Social behaviours are crucial for survival and reproduction across the animal kingdom and evolve dynamically throughout the lifespan based on social experiences.[1,2] For instance, adverse social experiences can lead animals to adopt a socially avoidant behavioural strategy aimed at reducing future harms and enabling access to essential resources through alternative routes.[3-5] However, clinically, intense social fear represents a common symptom observed in various mental disorders,[6] notably social anxiety disorder,[7] autism spectrum disorder[8] and schizophrenia.[9] Such behavioural maladaptation can lead to excessive and unnecessary social fear and avoidance behaviours even in a routine social context. Unfortunately, satisfactory treatment options for social fear remain inadequate because of a lack of understanding of how social trauma alters the neural system to give rise to social fear behaviour.

Accumulating studies have demonstrated a pivotal role of the medial prefrontal cortex (mPFC) in social behaviours, and mPFC dysfunction has been implicated in social deficits.[10-14] Previous human neuroimaging studies have shown hyperactivity and abnormal connectivity of the prefrontal cortex in social anxiety disorder patients.[15] Likewise, social stress significantly increases mPFC activity in rodents[16,17] and thus causes social fear behaviours. The mPFC implements higher-order brain functions through top-down control over its wide interconnectivity with subcortical regions.[18] For instance, the mPFC is known to process social information via its downstream brain regions, including the basolateral amygdala,[19] nucleus accumbens[20,21] and periventricular thalamus.[22] Nevertheless, little is known about how adverse social experiences impact the mPFC efferent pathways. Furthermore, the precise subcortical partners that mediate mPFC dysfunction on social fear behaviour are still unclear.

The lateral habenula (LHb) is often regarded as an 'anti-reward' centre[23] and receives afferent projections from the mPFC.[24] The LHb is known to be activated by various aversive stimuli, including foot shock, social stress and predator cues,[25,26] and plays a crucial role in the development of depressive-like behaviours induced by either physical or mental stressors.[27-29] Furthermore, there is evidence suggesting that the LHb is involved in the regulation of fear responses. For example, the presence of threatening looming stimuli greatly increases LHb activity that is necessary to elicit escaping behavioural responses.[30] Given the facts that the LHb lies downstream of the mPFC and has a direct impact on negative emotions, we hypothesized that the mPFC–LHb pathway participates in the regulation of social fear behaviour.

In the present study, we induced robust social fear with social fear conditioning[17,31-33] in mice and provide compelling evidence that the descending mPFC–LHb projection has a causal role in social fear behaviour. More importantly, using functional MRI (fMRI), we observed heightened prefrontal–habenular functional connectivity in populations with higher social anxiety. These data reveal a crucial role of the prefrontal–habenular circuitry in social fear regulation and suggest that the prefrontal–habenular pathway could serve as a potential target to ameliorate social fear symptoms associated with psychiatric disorders.

Materials and methods

Mice

All animal procedures were carried out according to the guidelines of the Animal Care and Use Committee of Zhejiang University. Adult male wild-type C57BL/6 mice and CaMKIIα-Cre mice[34] (Jackson stock no. 005359) at 8–16 weeks of age were used for experiments. Wild-type C57BL/6 mice were purchased from Shanghai Laboratory Animal Center. All mice were group housed until social fear conditioning or the social defeat procedure. Mice were maintained in standard housing conditions on a 12 h light–12 h dark cycle, with food and water *ad libitum*.

Virus injection and stereotactic surgeries

Mice were deeply anaesthetized with isoflurane (4% for induction, 1% for maintenance) and the head fixed in a stereotactic frame (Stoelting). Injections were performed with a 10 µl syringe (Hamilton) connected to a glass micropipette with a tip 20 µm in diameter. Syringe pumps (KdScientific) were used to inject the virus at a rate of 30 nl/min. The adeno-associated viruses (AAVs) described below were purchased from Taitool or BrainCase.

Fibre photometry

For recording LHb-projecting mPFC neurons, 100 nl of AAV2/9-hysn-DIO-GCaMP6m (a genetically encoded calcium indicator) (1.68×10^{12} virus genomes/ml) was injected unilaterally into the mPFC (relative to bregma: anteroposterior, +1.94 mm; mediolateral, ±0.40 mm; dorsoventral, −1.9 mm), and 30 nl of AAV-retro-hsyn-Cre-mCherry (1.0×10^{13} virus genomes/ml) was injected ipsilaterally into the LHb of C57 mice (relative to bregma: anteroposterior, −1.45 mm; mediolateral, ±0.46 mm; dorsoventral, −2.65 mm) at the same time. After the injection of viruses, a 200-µm-diameter, 0.37 NA optical fibre (Inper Technology) was implanted into the mPFC. For recording LHb neurons, 100 nl of AAV2/9-CaMKIIα-GCaMP6m (2.4×10^{12} virus genomes/ml) was injected unilaterally into the LHb of C57 mice (relative to bregma: anteroposterior, −1.45 mm; mediolateral, ±0.46 mm; dorsoventral, −2.65 mm), and an optical fibre was implanted into the LHb after viral injection.

Optogenetic manipulation

For stimulation of the mPFC–LHb projection in behavioural tests, 100 nl of AAV2/5-CaMKIIα-NpHR-EGFP (1.8×10^{12} virus genomes/ml) or 200 nl of AAV2/5-CaMKIIα-ChrimsonR-mCherry (2.0×10^{12} virus genomes/ml) was injected bilaterally into the mPFC of C57 mice (relative to bregma: anteroposterior, +1.94 mm; mediolateral, ±0.30 mm; dorsoventral, −1.9 mm). One hundred nanolitres of AAV2/5-CaMKIIα-EGFP (1.8×10^{12} virus genomes/ml) was injected bilaterally into the mPFC for the control group. Two weeks after viral injection, 200-µm-diameter, 0.37 NA optical fibres (Inper Technology) were implanted bilaterally into the LHb (relative to bregma: anteroposterior, −1.45 mm; mediolateral, ±0.83 mm; dorsoventral, −2.30 mm; 10° angle). For electrophysiological recording experiments, 200 nl of AAV2/9-hsyn-FLEX-ChrimsonR-tdTomato (2.0×10^{12} virus genomes/ml) was injected bilaterally into the mPFC of CaMKIIα-Cre mice (relative to bregma: anteroposterior, +1.94 mm; mediolateral, ±0.30 mm; dorsoventral, −1.9 mm).

Anterograde tracing

For anterograde tracing from mPFC to LHb, 100 nl of AAV2/5-CaMKIIα-EGFP (1.8×10^{12} virus genomes/ml) was injected unilaterally into the mPFC of C57 mice (relative to bregma: anteroposterior, +1.94 mm; mediolateral, ±0.30 mm; dorsoventral, −1.9 mm). Four weeks after virus infusion, the experimental mice were sacrificed.

Retrograde tracing

For retrograde tracing of LHb-projecting mPFC neurons, 30 nl of AAV-retro-hsyn-Cre-EGFP (6×10^{12} virus genomes/ml) was injected ipsilaterally into the LHb of C57 mice (relative to bregma: anteroposterior, −1.45 mm; mediolateral, ±0.46 mm; dorsoventral, −2.65 mm). Four weeks after virus infusion, the experimental mice were sacrificed.

Social fear conditioning

The conditioning apparatus was a square chamber (30 cm long × 30 cm wide × 50 cm high), with an electrical grid floor that provided a foot shock to the mice. Two fan-shaped (10 cm long × 10 cm wide × 25 cm high) transparent containers with holes distributed at the bottom of the container wall were placed diagonally in the conditioning apparatus. The chamber was cleaned with 75% ethanol before each trial.

Mice were singly housed for 5 days preceding the social fear conditioning procedure and were handled daily by the experimenter. The social fear conditioning was performed as described previously.[17,33] Briefly, on Day 1, mice were introduced to the social fear conditioning apparatus and permitted to explore the chamber freely for 10 min. On Day 2, after a 5 min period of free exploration, a stimulus mouse was introduced into one of the fan-shaped containers. After an additional 2 min of exploration, experimental mice received a brief foot shock (1 s, 0.5–0.6 mA) upon investigating the stimulus mouse during the subsequent 20 min. Twenty-four hours later, social fear behaviour was assessed by the three-chamber social interaction test or the social preference–avoidance test, as described below.

Our social fear conditioning protocol was adapted from the one proposed by Toth et al.[31] and Zoicas et al.[32] but with several significant modifications. First, instead of relying on visual inspection of social contacts and manual application of foot shocks, as described by Toth et al.[31] and Zoicas et al.,[32] we implemented an automated approach. Individual social investigation was detected, and electric shocks were delivered automatically using a computerized fear conditioning unit equipped with a video tracking system (Jiliang Software Technology). Social investigation was detected by the conditioning system when the following two criteria were met: (i) the distance between the nose of the experimental mouse and the centre of the stimulus mouse was no more than 4.5 cm; and (ii) the angle between the head direction of the experimental mouse and the line connecting the centre points of the two mice was no more than 45°. This modification aimed to ensure consistency in conditioning criteria and, consequently, reduce behavioural variation among conditioned subjects. Second, we adopted a set-up wherein two identical cages were placed at each of two opposing corners of the conditioning chamber. One cage remained empty, whereas the other contained a stimulus mouse. This arrangement was intended to facilitate fear acquisition specifically towards the stimulus mouse, rather than towards the cage itself. Notably, conditioned mice did not exhibit signs of fear towards the empty cage during or after conditioning. Third, we extended the duration of the conditioning procedure to 20 min, although experimental mice typically ceased investigating the stimulus mouse and receiving foot shocks after 5 min. This modification was inspired by findings indicating that maintaining physical proximity to a social stressor contributes to reinforcing behavioural adaptation, as observed in the social defeat paradigm.[35]

Subchronic social defeat

A 3-day subchronic social defeat stress procedure was performed as described previously.[36] An aggressive CD-1 mouse was introduced to the home cage of a singly housed adult male mouse for 15 min each day. The intruder was held in an acrylic enclosure during the first 5 min, and then allowed direct physical contact with the resident for the subsequent 10 min. Control mice were treated in the same way, except that the enclosure holding the CD-1 mice was not removed. Between 5 and 7 days after the last social defeat session, the experimental mice were subjected to fibre photometry recording.

Three-chamber social interaction test

The three-chamber apparatus was 60 cm long × 40 cm wide × 20 cm high and was evenly divided into three chambers by partitions, with openings 10 cm wide that allowed mice to pass freely. Two transparent cylindrical mouse containers (10 cm in diameter and 20 cm in height, with holes at the bottom of the wall allowing experimental mice to interact with and sniff stimuli mice) were placed at the distal corners of each side compartment. The testing process consisted of two 10 min phases. In the first phase, the experimental mice were placed in the middle chamber of the box and were allowed to explore the whole test box freely. In the second phase, unfamiliar stimuli mice of the same sex and age were randomly placed in one of the mouse containers, and the experimental mice were subjected to the box for another 10 min. The apparatus and mouse containers were cleaned with 50% ethanol after the test. Optical stimulation was delivered during the second interaction phase. The amount of time spent in each zone, the number of social investigations and the speed of movement were quantified during the second phase (EthoVision XT 11.5, Noldus). The social interaction index was calculated as the difference in the time spent in the social and neutral zones divided by the sum of the time spent in both zones. The mean duration of the investigation bout was calculated as the time spent in the social zone divided by the number of social zone investigations.

Social preference–avoidance test

The box was 42 cm long × 42 cm wide × 42 cm high, and a transparent cylindrical mouse container was placed in the centre of one side of the box. The testing process consisted of 10 min of free exploration and 10 min of social interaction. The box and mouse containers were cleaned with 50% alcohol after the test. Optical stimulation was delivered during the second interaction phase. The amount of time spent in each zone, the number of social investigations and the speed of movement were quantified during the second interaction phase (EthoVision XT 11.5, Noldus). The social interaction index was calculated as the time spent in the social zone divided by the time spent in corner zones. The mean duration was calculated as the time spent in the social zone divided by the number of social zone investigations. The percentage of stretched approaches was calculated as the fraction of stretched approaches among total approaches to the social zone.

Open field test

Mice were placed into the centre zone of an open field chamber (50 cm long × 50 cm wide × 50 cm high) for 10 min. The chamber was cleaned with 50% ethanol after the test. Optical stimulation was delivered during the whole session. The amount of time spent in the centre zone (25 cm × 25 cm) and the total distance of movement were quantified by EthoVision XT 11.5 (Noldus).

Real-time place preference test

The testing apparatus was 40 cm long × 40 cm wide × 20 cm high, separated into two chambers by a partition plate in the middle, with an opening 10 cm wide in the middle of the partition plate that allowed mice to pass freely. The testing process consists of two phases. In the first phase, mice were allowed to explore the whole test box freely for 20 min. In the second phase, mice were stimulated whenever they entered one selected chamber. Light stimulation paired chamber was randomly assigned and counterbalanced across mice, and a mini-IO box system was used to trigger the light (Noldus). The testing apparatus was cleaned with 50% ethanol after the test. The amount of time spent in each chamber was quantified by EthoVision XT 11.5 (Noldus).

Optogenetic manipulation in behavioural tests

Four weeks after virus infusion, experimental mice were introduced to behavioural testing. For optogenetic inhibition of mPFC–LHb pathway experiments, a 589 nm laser (Inper Technology) was used to deliver continuous light for 8 s followed by 2 s of light off, and the intensity of light delivered to the brain was 7–10 mW measured from the tip. For optogenetic activation of mPFC–LHb pathway experiments, a 635 nm laser (Inper Technology) was used to deliver light pulses for 15 ms, 10 Hz, and the intensity of light delivered to the brain was 4–6 mW measured from the tip. These parameters are consistent with previously validated and published protocols.[37-39]

Electrophysiological recordings

Four weeks after virus infusion, the experimental mice were anaesthetized and perfused with oxygen-saturated (95% O_2–5% CO_2) ice-cold artificial cerebrospinal fluid (ACSF; mM: 87 NaCl, 2.5 KCl, 1.25 NaH_2PO_4, 26 $NaHCO_3$, 1 $CaCl_2 \cdot 2H_2O$, 2 $MgSO_4 \cdot 7H_2O$, 75 sucrose and 10 glucose). The brain was quickly dissected and placed in oxygen-saturated cold ACSF, then sliced coronally (250 μm thickness) using a vibrating-blade microtome (Leica VT1200s). Brain slices containing mPFC and LHb nuclei were incubated in a holding chamber filled with high-sucrose ACSF at 32°C for 30 min. The brain slices were then transferred to standard ACSF (mM: 119 NaCl, 2.5 KCl, 1.25 NaH_2PO_4, 24 $NaHCO_3$, 2 $CaCl_2 \cdot 2H_2O$, 2 $MgSO_4 \cdot 7H_2O$ and 12.5 glucose) and incubated for ≥1 h at room temperature.

For cell recording, the brain slices were transferred to the recording chamber, which was continuously perfused with fully oxygenated standard ACSF at a rate of 2 ml/min. Whole-cell patch-clamp recordings were made using a MultiClamp 700B amplifier (Molecular Devices) and a 1440A digital-to-analog converter (Molecular Devices). The patch electrodes (3–7 MΩ resistance) used for recording were pulled by a P-97 puller (Sutter Instruments) and filled with an internal solution containing (mM: 130 potassium gluconate, 2 $MgCl_2 \cdot 6H_2O$, 5 KCl, 0.6 EGTA, 10 HEPES, 4 Mg-ATP and 0.3 Na-GTP, adjusted to pH 7.2–7.3; osmolality 285–290 mOsmol/kg).

To examine the efficiency of ChrimsonR expressed in mPFC calcium/calmodulin-dependent protein kinase II alpha (CaMKIIα)-positive neurons, the neurons were recorded in current-clamp mode and were given yellow light pulses at frequencies of 5, 10 and 20 Hz, respectively (3–5 mW, pulse width 2 ms), of each sweep. To record postsynaptic currents of mPFC excitatory neurons to LHb projections, a yellow light pulse (3–5 mW, pulse width 2 ms) was delivered to evoke presynaptic glutamate release from mPFC projections to the LHb, LHb neurons were held at −70 mV in voltage clamping mode, and neurons were again recorded for 10–30 sweeps. Tetrodotoxin (TTX, 1 μM, Sigma-Aldrich) and 4-aminopyridine (4-AP, 100 μM, Sigma-Aldrich) were used to prove that the mPFC–LHb pathway is a monosynaptic connection, and 6,7-dinitroquinoxaline-2,3-dione (DNQX, 10 μM, Sigma-Aldrich) and DL-2-amino-5-phosphonopentanoic acid (APV, 20 μM, Sigma-Aldrich) was used to prove that the mPFC–LHb pathway is an excitatory connection. To examine the efficiency of halorhodopsin (NpHR) in hyperpolarizing mPFC CaMKIIα neurons, the neurons were recorded in current-clamp mode with 0 or 150 pA current injection (duration 500 ms), and a yellow light (3–5 mW, duration 250 ms) was given during the current injection period.

Fibre photometry recording

The optical fibre used to guide the light between the fibre photometry system and the implanted optical fibre in experimental mice was often obstructed by the separate walls within the three-chamber arena. This obstruction not only posed technical challenges but also risked disrupting the behaviour of the experimental mice, potentially compromising the quality of our data. To circumvent these issues, we opted to perform the fibre photometry experiments in a social preference–avoidance test. This alternative experimental set-up allowed us to minimize potential disturbances and optimizing the quality of our data acquisition. The fibre photometry system (Thinker Tech Nanjing Biotech) was used to record the activity of LHb-projecting mPFC neurons and LHb neurons. Three weeks after virus injection, mice were subjected to social preference–avoidance behavioural tests. The behaviour of mice was recorded by using a top-view camera, and social interactions were manually annotated frame by frame. The intensity of light delivered to the brain was 20–40 μW measured from the tip. The calcium fluorescence change ($\Delta F/F$) values are calculated as $(F - F_0)/F_0$, where F_0 is the baseline fluorescence signal averaged over a 2 s control time window (from −5 s to −3 s) prior to the onset of each social interaction. The social interaction onset was defined as the moment when the experimental mouse initiated interaction with the stimulus mouse, when the distance between its nose and the mouse container ceased to decrease. A peri-event time histogram of $\Delta F/F$ aligned to the onset of social interaction was constructed for each animal, then averaged across animals. The area under the curve (AUC) was calculated as the sum of the fluorescence changes from −3 to 5 s in each social interaction trial. The peak value is the maximal value of the averaged calcium signal fluorescence change for each mouse. These analyses are consistent with previously studies.[40-42]

Functional MRI

Subjects

We recruited 103 participants from Zhejiang University between November 2021 and October 2022, and all reported no history of diagnosed social anxiety disorder based on The Diagnostic and Statistical Manual of Mental Disorders, Fifth Edition, and had not sought medical assistance owing to social anxiety complaints before. This study was approved by the Ethics Committee of Zhejiang University. Informed consent was obtained from each participant before the study, and all participants were compensated for their time.

The Liebowitz Social Anxiety Scale (LSAS)[43] was used to assess social anxiety. Given that our subjects are Chinese, we used a Chinese compilation of the LSAS to assess the social anxiety of subjects. It is validated in Chinese population and proved to be of high reliability and validity.[44] The LSAS has two subscales, the fear and

the avoidance subscales. Each subscale contains 13 social and 11 performance situations that are rated on separate four-point (from 0 = none to 3 = severe) scales. Given that the fear subscale and the avoidance subscale are highly correlated, which suggests significant redundancy between subscales,[45,46] only the fear sub-scale was used to quantify the level of social anxiety in the present study. We also used the brief symptom inventory to measure the level of anxiety and depression. The brief symptom inventory is a self-report instrument developed to assess psychological symptoms, which is used in a wide range of settings.[47]

Image acquisition

MRI data were acquired on a 3 T Siemens Prisma scanner using a 20-channel coil. The functional images were acquired using a T_2*-weighted gradient echo-planar imaging (EPI) sequence with multi-bands acceleration [multiband-factor = 4, repetition time (TR) = 1000 ms, echo time (TE) = 34 ms, flip angle = 50°, field of view (FOV) = 230 mm^2, matrix = 92 × 92, slice thickness = 2.50 mm, slice number = 52, voxel size = 2.50 mm × 2.50 mm × 2.50 mm]. High-resolution anatomical images were also collected for each participant using a T_1-weighted three-dimensional magnetization-prepared rapid gradient echo sequence (TR = 2300 ms, TE = 2.32 ms, flip angle = 8°, FOV = 240 mm^2, matrix = 256 × 256, slice thickness = 0.90 mm, slice number = 208, voxel size = 0.90 mm × 0.90 mm × 0.90 mm).

Data preprocessing

Resting-state fMRI analyses were performed using ANTs,[48] AFNI[49] and SPM12 (Wellcome Department of Cognitive Neurology). The fMRI pre-processing pipeline involved slice timing, head motion correction, segmentation, spatial normalization into an isotropic 2.5 mm^3 Montreal Neurological Institute template, smoothing (full-width at half-maximum = 6 mm), and band-pass filtering (0.01–0.1 Hz) for the smoothed data. All the fMRI data were checked for head motion and would be excluded if any of the six motion parameters was >3 mm.

Resting-state functional connectivity

Given that the ventral tegmental area (VTA) and habenula (Hb) were considered as counterparts for each with opposite functions, the VTA time series was included as a covariate to increase the specificity of Hb when performing voxel-wise multiple linear regression against social anxiety. Specifically, the Hb and VTA were depicted based on previous studies.[50,51] The resting-state functional connectivity of the Hb was represented by the beta coefficient, which was correlated with LSAS scores. Furthermore, based on prior knowledge about the 'social' brain map by meta-analysis of Neurosynth,[52] multiple comparisons were corrected within this 'social' map, leading to an uncorrected $P < 0.005$ and a minimal cluster size of 30 being considered as corrected $P < 0.05$ using 3dClustSim with AFNI.

Quantification and statistical analysis

Fluorescent images were collected by laser confocal microscopy (FV1200, Olympus). Quantification of fluorescent axon terminals was analysed in ImageJ. Quantification of retrograde tracing LHb-projecting mPFC neurons was counted manually. The boundaries of nuclei were identified according to the mouse brain atlas,[53] and outlines were labelled by Adobe Illustrator. Animal behaviours were videotaped and analysed by EthoVision XT 11.5 (Noldus) in the behavioural tests. No blinding was done in the animal experiments. Mice were pseudo-randomly assigned to unconditioned and conditioned groups or to the EGFP-expressing and ChrimsonR/NpHR

groups. Virus-injected mice with incorrect injection sites or incorrect locations of optical fibre tips were excluded.

Statistical parameters, including the exact value of n, precision measures [mean ± standard error of the mean (SEM)] and statistical significance are reported in the figures and the figure legends. Data are judged to be statistically significant when $P < 0.05$ by Student's t-test, two-tailed Mann–Whitney U-test, one-way ANOVA or two-way ANOVA. The non-parametric Spearman correlation coefficient was used to analyse the correlation of calcium fluorescent signals between LHb-projecting mPFC neurons and LHb neurons. Pearson's correlation coefficient was used to analyse the correlative relationship between LSAS scores and resting-state functional connectivity, and the partial correlation coefficient was used to adjust for age, sex, head motion, anxiety and depression. In figures, asterisks denote statistical significance (*$P < 0.05$, **$P < 0.01$, ***$P < 0.001$ and ****$P < 0.0001$) compared with controls. Statistical analysis was performed in GraphPad Prism v.9.

Results

The mPFC neurons are functionally connected with the LHb

Initially, we ascertained the direct innervation of LHb neurons by the mPFC inputs. Given that excitatory neurons constitute the primary projection neurons in mPFC, we infused an AAV containing EGFP under the control of CaMKIIα promotor (AAV-CaMKIIα-EGFP, 100 nl) into the mPFC to induce EGFP expression in excitatory neurons.[54-56] Consistent with previous studies,[55,57,58] we detected EGFP-labelled neuronal fibres across the entire LHb (Supplementary Fig. 1). Given that the cerebral cortex is a laminar structure composed of multiple layers, to clarify the laminar distribution of mPFC neurons projecting to the LHb, we then injected a retrograde tracing virus carrying EGFP (AAV-retro-hsyn-Cre-EGFP, 30 nl) into the LHb to label LHb-projecting mPFC neurons (Fig. 1A and B). Interestingly, we found that the EGFP-labelled LHb-projecting mPFC neurons were predominantly located in layer V (Fig. 1C), which contains output neurons projecting to subcortical regions.

Given the above-identified anatomical projections from the mPFC to the LHb, we next investigated the functional connectivity between these two brain regions. To achieve this, we expressed the ChrimsonR fused to tdTomato (AAV-hsyn-FLEX-ChrimsonR-tdTomato) in mPFC neurons of CaMKIIα-Cre mice (Fig. 1D and E). Using whole-cell current-clamp recordings, we observed that yellow light pulses reliably induced pulse-locked action potentials in the ChrimsonR-expressing mPFC neurons (Fig. 1F and G). This observation verified the efficacy of ChrimsonR expression in mPFC neurons. We then proceeded to determine whether mPFC neuronal axons make functional synaptic contacts with LHb neurons. Photostimulation of ChrimsonR-expressing mPFC axons in the LHb reliably evoked postsynaptic currents in recorded LHb neurons (Fig. 1H and I). Moreover, the postsynaptic currents were completely blocked by the voltage-gated sodium channel blocker TTX and were restored by additional bath application of the potassium channel blocker 4-aminopyridine. The above sequential synaptic responses indicated that the LHb neurons were directly innervated by the presynaptic axons originating from the mPFC neurons. Moreover, the restored postsynaptic currents were completely eliminated by the α-amino-3-hydroxy-5-methyl-4-isoxazolepropionic acid (AMPA) receptor antagonist 6,7-dinitroquinoxaline-2,3-dione and the N-methyl-D-aspartate (NMDA) receptor antagonist DL-2-amino-5-phosphonopentanoic acid (Fig. 1H and I). Together, these results
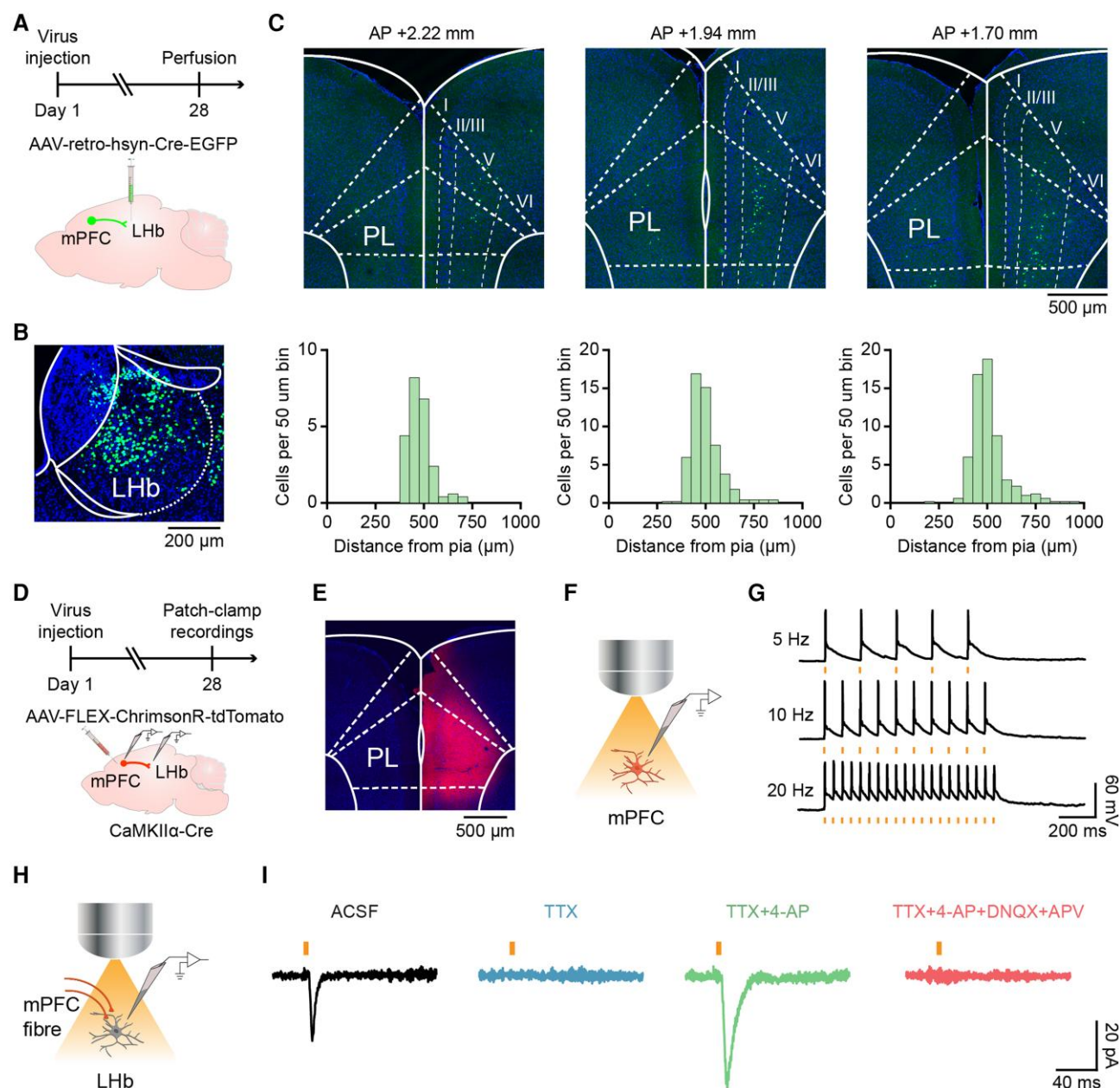
Figure 1 The mPFC neurons make monosynaptic connections with the LHb. (**A**) Schematic illustration of retrograde labelling of LHb-projecting mPFC neurons. (**B**) Representative image showing EGFP expression in LHb neurons. (**C**) Representative coronal sections showing retrogradely labelled prelimbic neurons along the anterior–posterior axis (*upper panels*) and corresponding cell counts from pia to white mater (data are expressed as the mean value, *n* = 5 mice, bin = 50 μm; *lower panels*). (**D**) Schematic diagram of the electrophysiological recordings from mPFC and LHb neurons. (**E**) Representative image showing ChrimsonR-tdTomato expression in the mPFC. (**F**) Schematic diagram of current-clamp recording from mPFC tdTomato⁺ neurons. (**G**) Brief yellow light pulses at 5, 10 and 20 Hz reliably activated ChrimsonR-expressing neurons in the mPFC. The yellow lines indicate the light delivery. (**H**) Schematic diagram of voltage-clamp recording from LHb neurons. (**I**) Representative postsynaptic current traces recorded from LHb neurons by optical stimulation of prefrontal fibres in the LHb in sequence of bath application of ACSF, TTX, TTX + 4-AP and TTX + 4-AP + DNQX + APV. ACSF = artificial cerebrospinal fluid; 4-AP = 4-aminopyridine; APV = ᴅʟ-2-amino-5-phosphonopentanoic acid; DNQX = 6,7-dinitroquinoxaline-2,3-dione; EGFP = enhanced green fluorescent protein; LHb = lateral habenula; mPFC = medial prefrontal cortex; TTX = tetrodotoxin.

demonstrated that deep-layer mPFC neurons established monosynaptic glutamatergic contacts with LHb neurons.

The LHb-projecting mPFC neurons are activated during social fear expression

To investigate the involvement of the mPFC–LHb pathway in social fear behaviours, we measured the activities of LHb-projecting mPFC neurons directly using fibre photometry (Fig. 2A). Initially, we induced social fear responses in mice through the social fear conditioning paradigm, as previously described.[17] In brief, a freely moving experimental mouse received a mild foot shock when it investigated a stimulus mouse. Subsequently, social fear behaviours were quantified with a social preference–avoidance test (Supplementary Fig. 2A). On average, the experimental mice ceased investigating the conspecific after receiving around four foot

shocks during the conditioning session. (Supplementary Fig. 2B and C). In comparison to unconditioned control mice, conditioned mice spent dramatically less time in the social zone, huddled more in the corner zone, exhibited a lower social index, initiated fewer social approaches, had shorter investigation duration and approached the stimulus mice with slower speed and more stretched postures (Supplementary Fig. 2D–J). These behavioural manifestations indicated that conditioned mice exhibited robust social fear behaviours in response to social stimuli.

To record the activity of LHb-projecting mPFC neurons, we injected a retrogradely transported virus (AAV-retro-hsyn-Cre-mCherry) into the LHb and a Cre-dependent calcium indicator virus (AAV-hsyn-DIO-GCaMP6m) into the mPFC, which brought about the expression of GCaMP6m in the mPFC–LHb projection neurons. Then, we implanted an optical fibre (~200 μm in diameter) in the mPFC to record the calcium-dependent fluorescent signals (Fig. 2B and C). Three weeks after virus infusion, we conducted social fear conditioning on the mice. In the social preference–avoidance test, we found that the Ca²⁺ signals of LHb-projecting mPFC neurons remained unchanged when unconditioned mice interacted with social stimuli in the social zone (Fig. 2D and E). In striking contrast, a large increase in Ca²⁺ signals was observed in LHb-projecting mPFC neurons when conditioned mice encountered the social stimulus (Fig. 2F and G). Statistically, both the peak amplitude (unconditioned: $5.22 \pm 1.03\%$, $n = 7$; conditioned: $10.42 \pm 1.43\%$, $n = 8$; $P < 0.05$) and the AUC (unconditioned: 10.24 ± 6.25, $n = 7$; conditioned: 39.34 ± 6.40, $n = 8$; $P < 0.01$) of Ca²⁺ signals were significantly larger in conditioned mice compared with unconditioned mice (Fig. 2H and I). These observations indicated that the elevated activity of mPFC–LHb neurons was associated with social fear responses.

We also measured the activity of LHb-projecting mPFC neurons in mice with social fear induced by another well-established paradigm, i.e. the subchronic social defeat paradigm.[4,36] Following 3 days of repeated social defeat, the defeated mice exhibited social fear behaviours, as revealed in the social preference–avoidance test (Supplementary Fig. 3A–E). The Ca²⁺ signals of LHb-projecting mPFC neurons remained unchanged when undefeated control mice interacted with the social stimulus, but the Ca²⁺ signals showed a large increase when the defeated mice encountered the social stimulus (Supplementary Fig. 3I–L). Both the peak amplitude and the AUC of Ca²⁺ signals were significantly larger in defeated mice compared with undefeated control mice (Supplementary Fig. 3M and N). These results indicated that the LHb-projecting mPFC neurons were activated during social fear expression in our experimental paradigms.

The activity of LHb neurons increases during social fear expression

The foregoing experiments suggested that the hyperactivity of the mPFC–LHb projection is likely to be linked to social fear behaviours. Next, we therefore examined the response of LHb neurons upon expression of social fear (Fig. 3A). To do this, we infused a virus encoding the calcium indicator GCaMP6m (AAV-CaMKIIα-GCaMP6m) in the LHb and implanted an optical fibre to monitor the calcium fluorescent signals of LHb neurons (Fig. 3B and C). In the social preference–avoidance test, there was a minimal change in calcium fluorescent signals in LHb neurons when unconditioned control mice interacted with the social stimulus (Fig. 3D and E). Notably, in conditioned mice, the onset of social contact was accompanied by a large increase in calcium fluorescent signals in LHb neurons (Fig. 3F and G). Statistically, both the peak amplitude

(unconditioned: $7.17 \pm 0.76\%$, $n = 5$; conditioned: $21.36 \pm 2.33\%$, $n = 7$; $P < 0.001$) and the AUC (unconditioned: 12.28 ± 4.96, $n = 5$; conditioned: 63.92 ± 10.21, $n = 7$; $P < 0.01$) of calcium fluorescent signals in the conditioned mice were significantly larger than those in the unconditioned mice (Fig. 3H and I). Therefore, the activity of LHb neurons was also elevated in response to the social stimulus in conditioned mice. This set of data is consistent with our previous observation showing activation of the mPFC–LHb pathway during social fear expression (Fig. 2).

Prefrontal and LHb activities become highly synchronized during social fear expression

Given that the activities of LHb-projecting mPFC neurons and LHb neurons were both increased during social fear expression, we wondered whether the mPFC implements its function in social fear via its downstream LHb. To test this, we initially investigated the interregional correlation of neuronal activity between the mPFC and the LHb during social fear expression. We adopted a dual-site fibre photometry strategy to record the calcium fluorescent signals of LHb-projecting mPFC neurons and LHb neurons simultaneously in a social preference–avoidance test (Fig. 4A). Specifically, we infused a virus encoding a calcium indicator (AAV-CaMKIIα-GCaMP6m) and a retrograde AAV-retrovirus encoding Cre recombinase (AAV-retro-hsyn-Cre-mCherry) into the LHb and a Cre-dependent virus encoding a calcium indicator (AAV-hsyn-DIO-GCaMP6m) into the mPFC, then implanted optical fibres in the mPFC and the LHb, respectively (Fig. 4B and C). We found that these two populations of neurons displayed apparently synchronized activities when the conditioned mouse investigated a stimulus mouse but not an empty cage (Fig. 4D). Therefore, we analysed the correlation of the calcium fluorescent signals between the LHb-projecting mPFC neurons and the LHb neurons during individual investigation bouts. Compared with the empty cage investigation, a significantly stronger correlation was observed when conditioned mice investigated a stimulus mouse (cage interaction: 0.14 ± 0.05; social interaction: 0.43 ± 0.06; $n = 8$; $P < 0.001$; Fig. 4D–F). These observations indicate that the prefrontal and lateral habenular activities became highly synchronized during social fear expression.

Optogenetic inhibition of the mPFC–LHb projection reduces social fear responses

Aberrant activation of the mPFC is tightly linked to social fear expression.[17] Here, both the elevated activity of the LHb-projecting mPFC neurons (Fig. 3) and the heightened correlation between prefrontal and LHb activities (Fig. 4) during social fear expression further suggest that the mPFC could implement its function in social fear via its downstream LHb. To test this, we first examined the impact of direct activation of the mPFC–LHb pathway on social behaviours in naïve mice with a three-chamber social interaction test. Specifically, we delivered an optogenetic virus expressing ChrimsonR or EGFP under the control of CaMKIIα promotor (AAV-CaMKIIα-ChrimsonR-mCherry or AAV-CaMKIIα-EGFP) into the mPFC and implanted optical fibres bilaterally in the LHb (Supplementary Fig. 4A and B). Four weeks after virus infusion, we subjected the mice to the social interaction test; a stimulus mouse was placed randomly in one of the mouse containers (Supplementary Fig. 4C). Following red light (635 nm) stimulation through the optical fibres implanted in the LHb, mice expressing ChrimsonR spent significantly less time in the social zone,
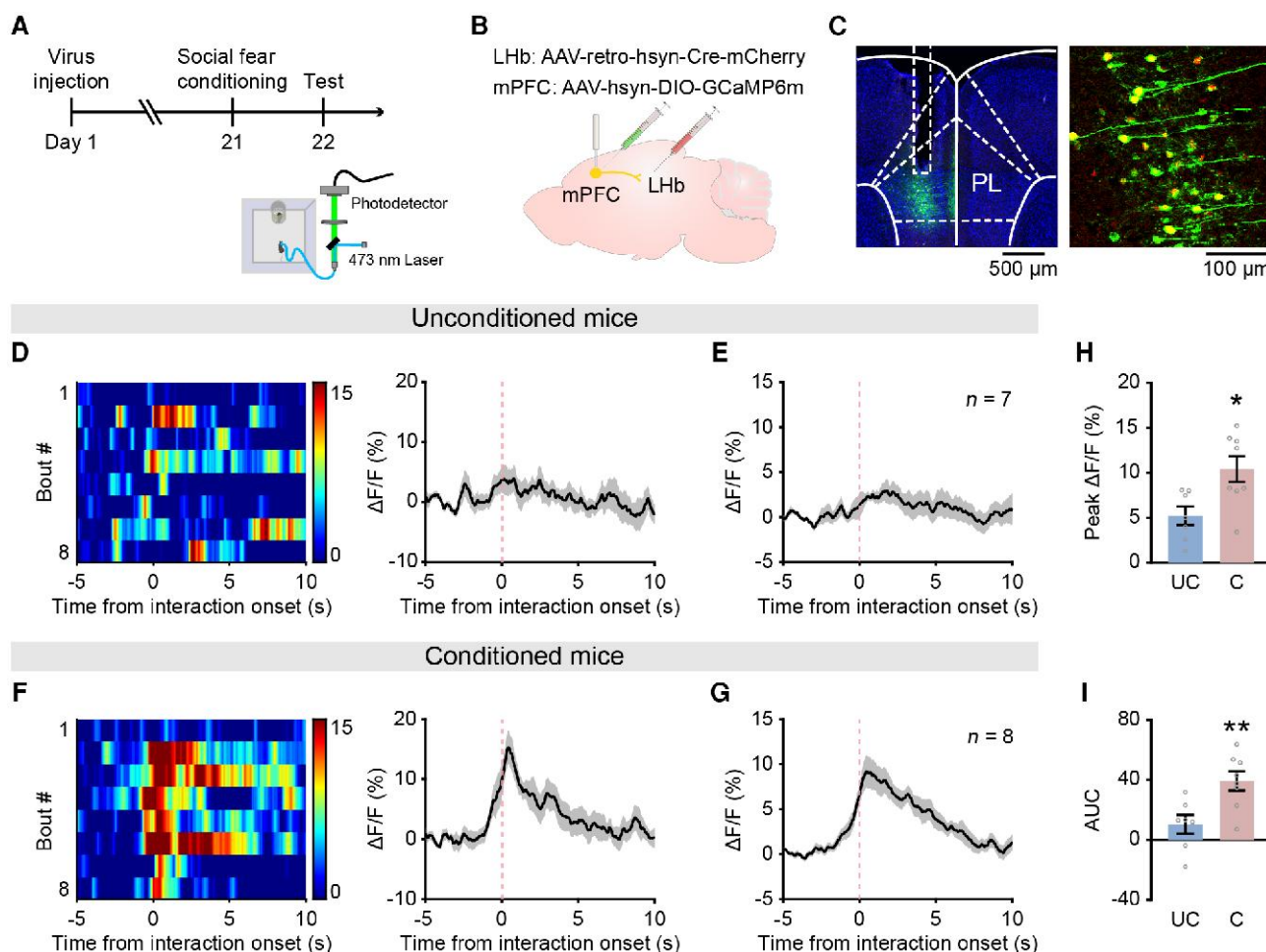
Figure 2 The activity of LHb-projecting mPFC neurons is highly elevated during social fear expression. (**A**) Schematic diagram of fibre photometry recording of the calcium fluorescent signals from LHb-projecting mPFC neurons in a social preference–avoidance test. (**B**) Schematic illustration of the viral strategy for recording LHb-projecting mPFC neurons. (**C**) Representative images showing optical fibre placement in the mPFC (*left*) and GCaMP6m expression in LHb-projecting mPFC neurons (*right*). (**D**) The calcium fluorescent signals of LHb-projecting mPFC neurons in the social preference–avoidance test from an unconditioned control mouse. Heat map representations (*left*) and averaged peri-event plot (*right*) of ΔF/F ratio of calcium fluorescent signals aligned to social interaction onset. The thick black line indicates the mean, and shaded area indicates the standard error of the mean (SEM). (**E**) Mean calcium responses of LHb-projecting mPFC neurons aligned to interaction onset from unconditioned control mice ($n = 7$ mice). (**F** and **G**) The same as **D** and **E**, but for mice with conditioned social fear ($n = 8$ mice). (**H** and **I**) Statistical comparison of peak amplitudes (**H**) and AUC (**I**) between unconditioned and conditioned mice (Student's unpaired *t*-test). Data are expressed as the mean ± SEM, *$P < 0.05$ and **$P < 0.01$. AUC = area under the curve; C = conditioned; LHb = lateral habenula; mPFC = medial prefrontal cortex; UC = unconditioned.

exhibited a reduced social interaction index and engaged in fewer social approaches in comparison to EGFP-expressing control mice (Supplementary Fig. 4D–H). These results suggested that activation of the mPFC–LHb pathway reduced social behaviours in naïve mice.

Given that the emotional states of the animals could have an impact on their social behavioural output,[59] we therefore assessed whether activation of the mPFC–LHb pathway would induce an aversive effect. To address this, we subjected naïve mice to a real-time place avoidance test, and red light was delivered each time the experimental mice entered the randomly assigned light-on chamber. We found that both EGFP-expressing mice and ChrimsonR-expressing mice spent statistically equal amounts of time in the light-on and light-off chambers during both the free exploration phase and the light stimulation phase (Supplementary Fig. 4I–K). These results indicate that activation of the mPFC–LHb pathway did not elicit place aversion and suggest that hyperactivity of the mPFC–LHb pathway was sufficient to produce social avoidance behaviour.

To determine whether hyperactivity of the mPFC–LHb pathway plays a causal role in social fear behaviour, we used optogenetics to inhibit this pathway selectively. Specifically, we expressed halorhodopsin (eNpHR3.0) or EGFP under the control of the CaMKIIα promotor (AAV-CaMKIIα-NpHR-EGFP or AAV-CaMKIIα-EGFP) in mPFC neurons and implanted optical fibres bilaterally in the LHb (Fig. 5A and B). We assessed the efficacy of NpHR-mediated inhibition through *ex vivo* patch-clamp recordings from mPFC neurons and found that yellow light stimulation (589 nm) successfully induced hyperpolarization in NpHR-expressing mPFC neurons and completely suppressed their action potentials evoked by current injections (Fig. 5C). Four weeks after virus infusion, we subjected the mice to social fear conditioning. We then optogenetically inhibited mPFC axon terminals in the LHb during social fear expression examined with a three-chamber social interaction test (Fig. 5D). In comparison to the EGFP-expressing control mice, the NpHR-expressing mice spent significantly more time in the social zone (EGFP: 20.09 ± 6.80 s, $n = 14$; NpHR: 75.29 ± 15.56 s, $n = 14$; $P < 0.01$), exhibited a significant increase in the social
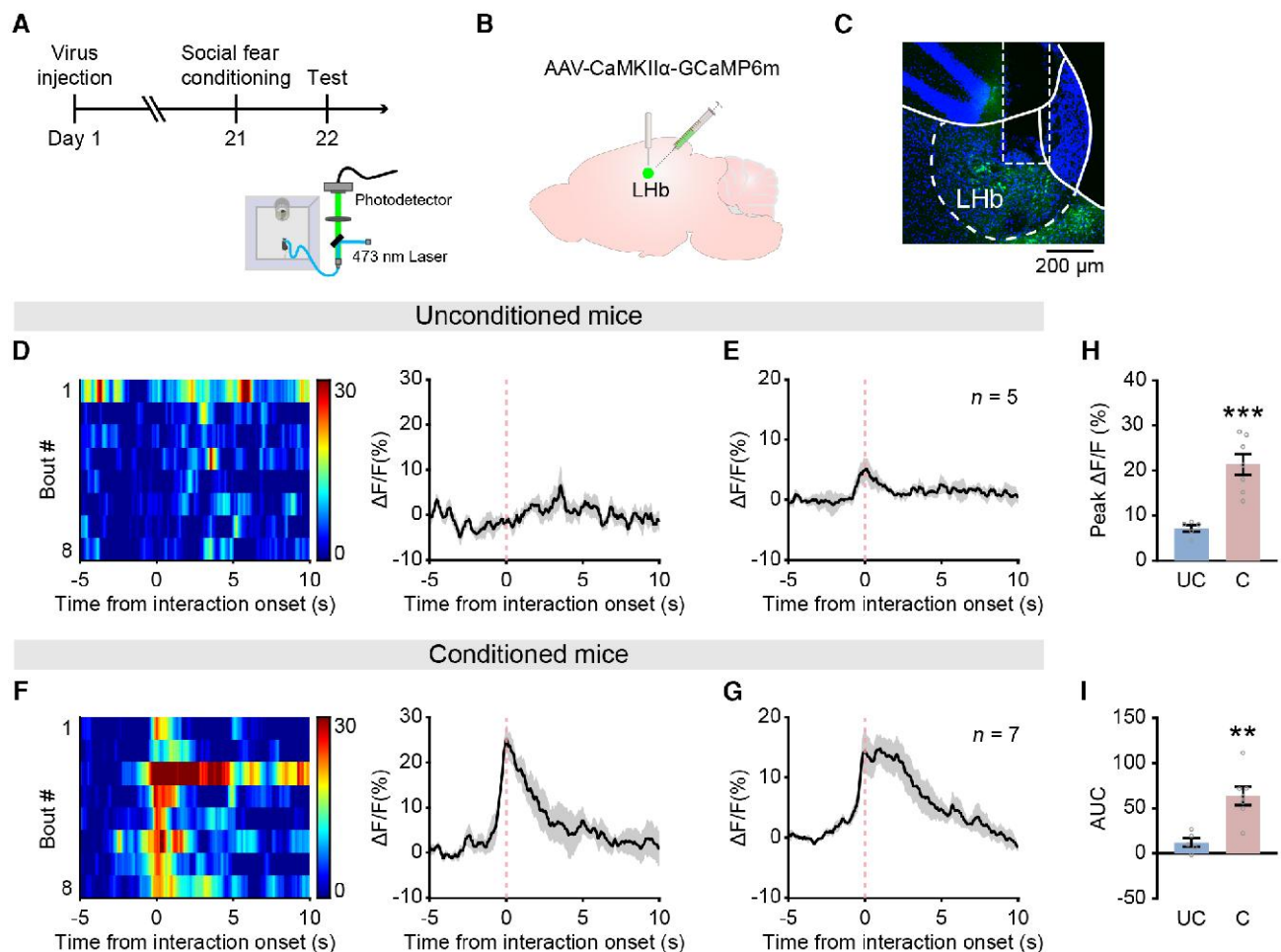
Figure 3 The activity of LHb neurons is highly elevated during social fear expression. (**A**) Schematic diagram of fibre photometry recording of the calcium fluorescent signals from LHb neurons in a social preference–avoidance test. (**B**) Schematic illustration of the viral strategy for recording LHb neurons. (**C**) Representative images showing GCaMP6m expression and optical fibre placement in the LHb neurons. (**D**) The calcium fluorescent signals of LHb neurons in the social preference–avoidance test from an unconditioned mouse. Heat map representations (*left*) and averaged peri-event plot (*right*) of ΔF/F ratio of calcium fluorescent signals aligned to social interaction onset. The thick black line indicates the mean, and the shaded area indicates the standard error of the mean (SEM). (**E**) Mean calcium responses of LHb neurons ratio aligned to interaction onset from unconditioned control mice ($n = 5$ mice). (**F** and **G**) The same as **D** and **E**, but for mice with conditioned social fear ($n = 7$ mice). (**H** and **I**) Statistical comparison of peak amplitudes (**H**) and AUC (**I**) between unconditioned and conditioned mice (Student's unpaired t-test). Data are expressed as the mean ± SEM, $^{**}P < 0.01$ and $^{***}P < 0.001$. AUC = area under the curve; C = conditioned; LHb = lateral habenula; UC = unconditioned.

interaction index (EGFP: -0.69 ± 0.07, $n = 14$; NpHR: -0.25 ± 0.12, $n = 14$; $P < 0.01$), engaged in more social approaches (EGFP: 4.86 ± 1.33, $n = 14$; NpHR: 11.21 ± 1.10, $n = 14$; $P < 0.01$) and had a longer mean duration of investigation (EGFP: 3.83 ± 0.39 s, $n = 14$; NpHR: 6.00 ± 0.95 s, $n = 14$; $P < 0.05$) (Fig. 5E–I). Together, these results demonstrated that inhibition of the mPFC–LHb pathway increased the social interaction time in mice with conditioned social fear, suggesting a reduction of social fear behaviour.

In addition to a reduction of social fear, the observed increase in social investigation after inhibition of the mPFC–LHb pathway could also reflect an alteration in the emotional state or sociability of an animal.[60] Therefore, we initially evaluated the impact of the mPFC–LHb pathway inhibition on anxiety-like behaviour in mice with conditioned social fear using an open field test. Both EGFP-expressing mice and NpHR-expressing mice spent a similar amount of time in the central area and travelled similar distances in the open field (Supplementary Fig. 5C–E). These results suggest that inhibition of the mPFC–LHb pathway did not influence the anxiety level or locomotion of the animal. Moreover, inhibition of the mPFC–LHb pathway did not induce an

appetitive response in mice with conditioned social fear in a real-time place preference test (Supplementary Fig. 5F–H). To determine whether inhibition of the mPFC–LHb pathway increases basal sociability, we next adopted an optogenetic strategy to inhibit this pathway in unconditioned control mice and examined its consequence on the sociability of animals. We found that inhibition of the mPFC–LHb pathway did not alter the time spent in the social zone (Supplementary Fig. 6). This finding indicated that this manipulation did not compromise the capability of animals to differentiate other subjects or promote social preference non-specifically. Taken together, these results demonstrated that the hyperactivity of the mPFC–LHb pathway is necessary for social fear behaviour in conditioned mice.

Social anxiety trait is correlated with the prefrontal–habenular functional connectivity in human subjects

The above-mentioned studies clearly revealed the importance of the mPFC–LHb pathway for social fear regulation in mice with
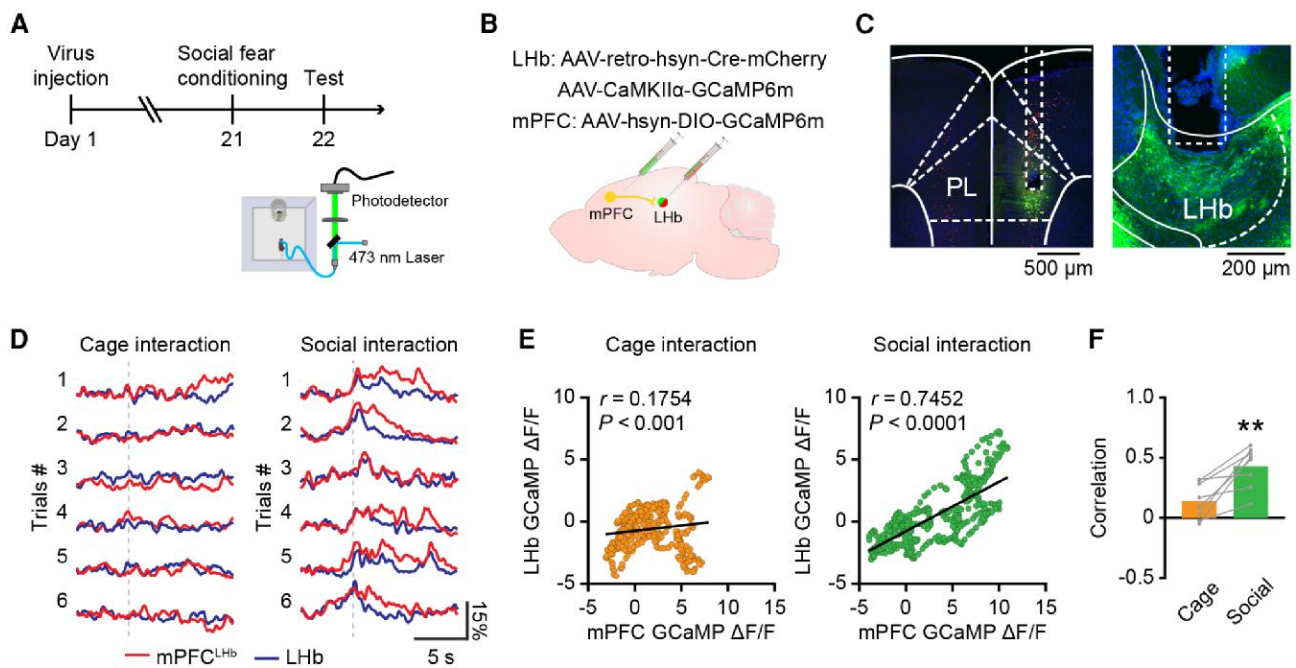
Figure 4 The activities of LHb-projecting mPFC neurons and LHb neurons become highly synchronized during social fear expression. (**A**) Schematic diagram of fibre photometry recordings of the calcium fluorescent signals from both LHb-projecting mPFC neurons and LHb neurons during the social preference–avoidance test. (**B**) Schematic illustration of the viral strategy for recording both LHb-projecting mPFC neurons and LHb neurons. (**C**) Representative images showing GCaMP6m expression and optical fibre placement in the mPFC (*left*) and the LHb (*right*). (**D**) Representative calcium signals of LHb-projecting mPFC neurons (*red*) and LHb neurons (*blue*) when a conditioned mouse investigated an empty cage (*left*) and a social stimulus (*right*) during the social preference–avoidance test. (**E**) The correlation between calcium signals of LHb-projecting mPFC neurons and those of LHb neurons in a single event of empty cage exploration (*left*) and social interaction (*right*) (Spearman correlation coefficient). (**F**) The activities of LHb-projecting mPFC neurons and LHb neurons were more correlated during social interaction than cage interaction in mice with conditioned social fear ($n = 8$, Student's paired t-test). Data are expressed as the mean ± standard error of the mean, **$P < 0.01$. LHb = lateral habenula; mPFC = medial prefrontal cortex.

conditioned social fear. Next, it was essential to determine the involvement of the prefrontal–habenular pathway in human subjects. For this purpose, we recruited 103 college students from Zhejiang University and administrated an 8 min resting-state fMRI scan (for data quality control, see Supplementary Table 1). Their trait-like social anxiety was assessed using the LSAS, a well-established measurement of social anxiety.[43]

Initially, a meta-analysis was performed using the term 'social' in Neurosynth (https://github.com/neurosynth/neurosynth) to identify brain areas related to social processing. The results confirmed the involvement of several regions in the social brain network, including the ventromedial prefrontal cortex, the dorsomedial prefrontal cortex, the posterior cingulate cortex and the temporoparietal junction (Fig. 6A).

Next, functional connectivity was calculated using the entire Hb as the seed region, and this region was regarded as a surrogate for the mouse LHb because the resolution of our fMRI (2.50 mm × 2.50 mm × 2.50 mm for fMRI) did not allow an accurate separation of Hb subregions. Based on Student's one-sample t-test, the Hb exhibited a positive resting-state functional connectivity with the dorsomedial prefrontal cortex, posterior cingulate cortex, temporoparietal junction, cerebellum, thalamus, ventromedial prefrontal cortex and the cingulate cortex (Fig. 6B). These observations are consistent with a previous study mapping the detailed functional connectivity of the habenula across the brain.[61]

To examine the relationship between Hb connectivity and social anxiety, a regression analysis of Hb connectivity against social anxiety was performed within the social network (i.e. Fig. 6A). The results, corrected for multiple comparisons (corrected $P < 0.05$),

revealed that the resting-state functional connectivity of the dorsomedial prefrontal cortex–Hb pathway was positively correlated with the score on LSAS ($r = 0.326$, $P = 0.001$; Fig. 6C and D). Other clusters connected functionally with the Hb, including the right temporoparietal junction and the posterior cingulate cortex, also showed a significant correlation with LSAS scores (right temporoparietal junction, $r = 0.370$, $P < 0.001$; posterior cingulate cortex, $r = 0.366$, $P < 0.001$; Fig. 6C and D). These analyses suggest an essential role of the Hb in regulating self-oriented social and negative emotion processing, because those regions are part of the default mode network. In particular, when the influences of age, sex, head motion, anxiety and depression were controlled, the partial correlation between social anxiety and the functional connectivity of the dorsomedial prefrontal cortex–Hb pathway remained significant (dorsomedial prefrontal cortex–Hb: $r = 0.289$, $P = 0.004$). Taken together, these analyses revealed a tight link between the prefrontal–habenula functional connectivity and the level of social anxiety in human subjects. This set of data uncovers an elevated prefrontal–habenular functional connectivity in subclinical individuals with higher social anxiety characterized by heightened social fear.

Discussion

In the present study, combining fibre photometry and pathway-specific activity manipulation, we found that the mPFC–LHb pathway is highly activated during social fear expression in mice. Moreover, inhibition of this pathway is sufficient to reduce social fear responses to stimulus mice. Furthermore, using resting-state
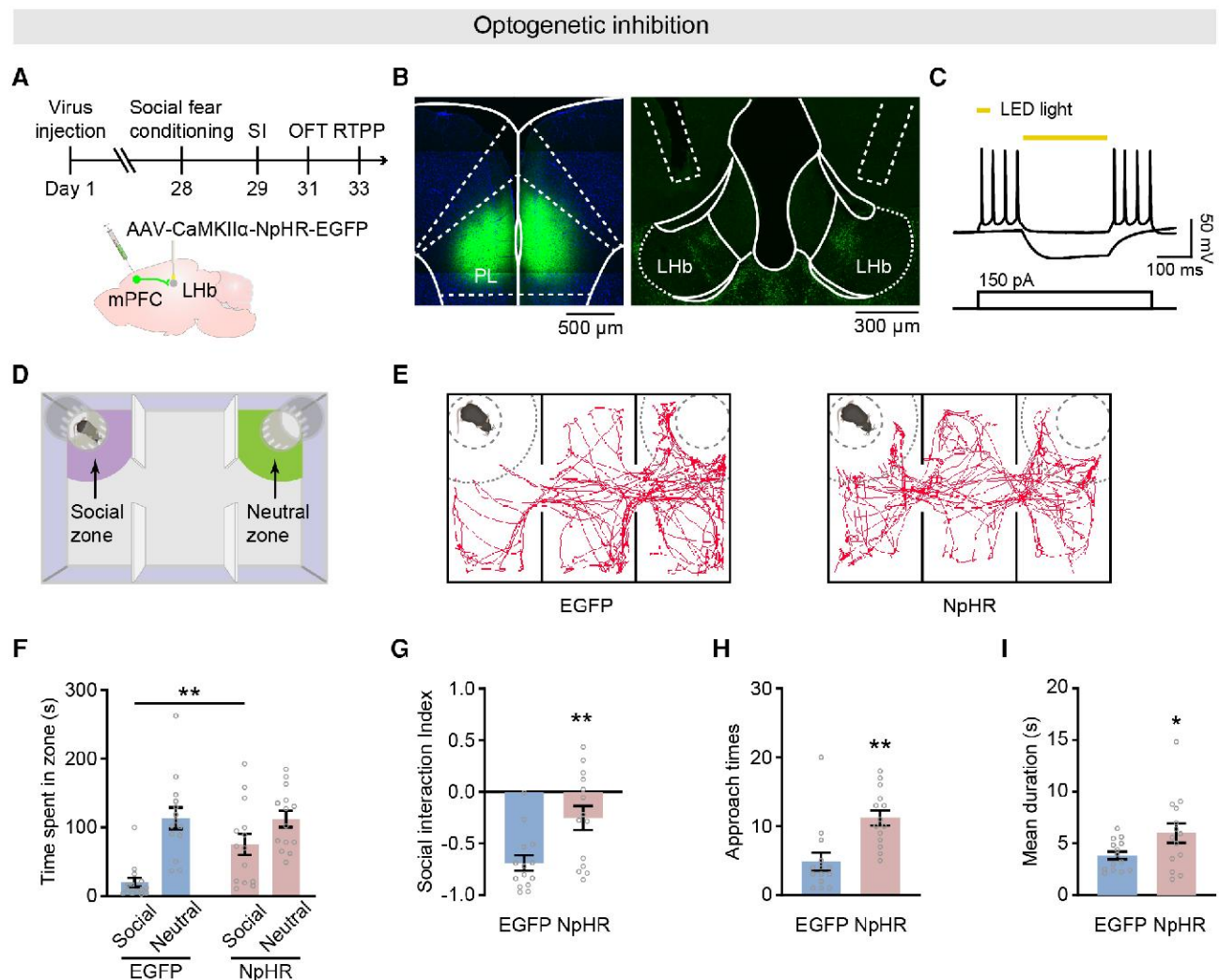
Figure 5 Optogenetic inhibition of the mPFC–LHb pathway reduces social fear responses. (**A**) Schematic illustration of the viral strategy for mPFC–LHb pathway inhibition. The adeno-associated virus carrying NpHR was injected into the mPFC, and the optical fibre was implanted in the LHb. (**B**) Representative images showing NpHR expression in mPFC neurons (*left*) and optical fibre placement in the LHb (*right*). (**C**) Representative traces showing that yellow light induced a large hyperpolarization of an NpHR-expressing mPFC neuron. Light delivery is indicated by the yellow bar. (**D**) Schematic illustration of three-chamber social interaction test. (**E**) Representative movement traces of EGFP-expressing and NpHR-expressing mice in the three-chamber social interaction test following light stimulation. (**F**) Quantification of time spent in the social and neutral zone in the three-chamber social interaction test ($n = 14$ for EGFP-expressing mice, $n = 14$ for NpHR-expressing mice, two-way ANOVA, Bonferroni multiple comparison *post hoc* tests). (**G**) The social interaction index (the difference in the time spent in the social and neutral zones divided by the sum of the time spent in both zones) of EGFP-expressing and NpHR-expressing mice (Student's unpaired *t*-test). (**H** and **I**) Comparison of social approach times (**H**) and mean duration of social investigation bouts (**I**) in EGFP-expressing mice and NpHR-expressing mice in the three-chamber social interaction test (Student's unpaired *t*-test). Data are expressed as the mean ± standard error of the mean, *$P < 0.05$ and **$P < 0.01$. EGFP = enhanced green fluorescent protein; LHb = lateral habenula; mPFC = medial prefrontal cortex; NpHR = halorhodopsin; SI = social interaction test; OFT = open field test; RTPP = real-time place preference test.

fMRI, we observed that prefrontal–habenular functional connectivity is positively correlated with social anxiety level in human subjects. These data unravelled a causal role of the prefrontal–habenular circuitry in social fear regulation and suggest that this pathway could serve as a therapeutic target to ameliorate social fear symptoms in related disorders.

The LHb-projecting prefrontal neurons underlie social fear behaviour

Like other cortices, the mPFC is a layered structure,[62] and each layer contains distinct populations of pyramidal neurons projecting to diverse subcortical targets.[63] For example, the basolateral amygdala, an area essential for emotion regulation,[64] receives innervations from the supragranular layers 2/3.[20] In comparison, the paraventricular thalamus and the mediodorsal thalamus mainly receive mPFC afferents arising from infragranular layer 6.[63,65,66] Unlike those subcortical regions, our retrograde tracing revealed that the mPFC neurons projecting to the LHb were predominantly located in layer 5 (Fig. 1C). This anatomical organization suggests that the mPFC neurons transform cortical information to the LHb and other brain regions, hence they execute distinct functions in a layer-dependent manner.

The prefrontal cortex has long been implicated in the regulation of fear responses acquired through classical Pavlovian conditioning.[64,67,68] With the aid of neural circuit tracing and pathway-specific manipulation, recent studies have started to dissect mPFC long-range circuits underlying learned fear behaviour.[69,70]
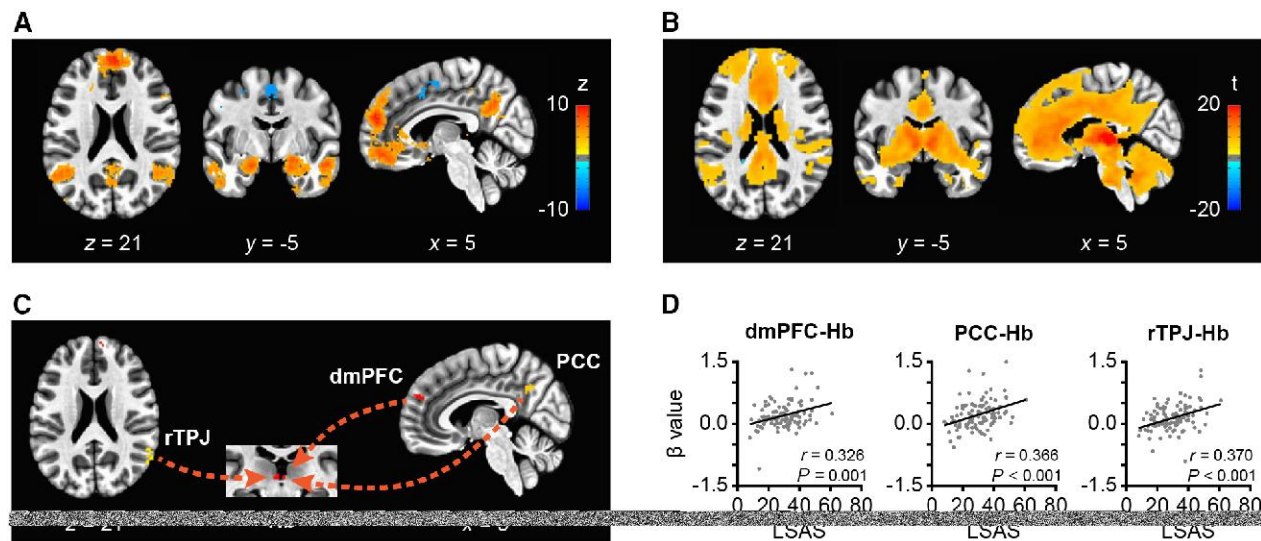
Figure 6 Social anxiety trait is correlated with the prefrontal–habenular functional connectivity in human subjects. (**A**) The social brain network identified by meta-analyses. (**B**) The resting-state functional connectivity pattern of Hb (Student's one-sample *t*-test, corrected $P < 0.00001$). (**C**) Brain regions whose functional connectivity with the Hb showed significant correlations with social anxiety characterized by the LSAS score (corrected $P = 0.05$). Arrows are for illustrative purposes and do not indicate directionality. (**D**) Scatterplots showing the correlation between the LSAS score and the resting-state functional connectivity of the three Hb-seeded pathways. dmPFC = dorsomedial prefrontal cortex; Hb = habenula; LSAS = Liebowitz Social Snxiety Scale; PCC = posterior cingulate cortex; rTPJ = right temporoparietal junction.

For instance, it is now known that the freezing response induced by conditioning stimulus is under control of prefrontal projection onto the basolateral amygdala, periaqueductal grey (PAG) or periventricular thalamus.[71,72] Here, we report, for the first time and based on several lines of evidence, that the descending mPFC–LHb projection has a crucial role in conditioned social fear behaviour in mice. First, we demonstrated with fibre photometry that both the LHb neurons and the LHb-projecting mPFC neurons were robustly activated by a social stimulus in conditioned mice (Figs 2 and 3). Second, with simultaneous dual fibre photometry recordings, we showed that the neuronal activity of the LHb neurons and the LHb-projecting mPFC neurons were highly correlated during social fear expression (Fig. 4). Third, selective inhibition of the mPFC–LHb projection with optogenetics significantly reduced social fear responses in conditioned mice (Fig. 5). Together, these results support a causal role of the descending mPFC–LHb projection in conditioned social fear behaviour in mice.

As mentioned above, the mPFC neurons also project to the PAG, and the mPFC–dorsal PAG (dPAG) pathway also plays a role in social fear behaviour.[36] Interestingly, like the LHb-projecting mPFC neurons, the dPAG-projecting mPFC neurons are also specifically located in layer 5. However, in contrast to the mPFC–LHb pathway, social defeat weakened the functional connectivity of the mPFC–dPAG pathway, and inhibition of the mPFC–dPAG pathway induced social avoidance in naïve mice. Therefore, it seems that the mPFC–LHb pathway and the mPFC–dPAG pathway operate in an opposite way in response to adverse social experiences. In addition to the dPAG, the lateral hypothalamus also receives neuronal projections from mPFC layer 5. In this case, it is the increased neuronal excitability of the mPFC–lateral hypothalamus pathway that contributes to social deficits.[73] Taken together, these results suggest that prefrontal neurons, even within the same layer, could regulate social fear behaviour by targeting different subcortical partners in different ways. Given the complexity of social behaviours that are under instantaneous influence of both sensory cues and internal states of the animal,[10,74-76] prefrontal neurons projecting to multiple targets

need to act synergistically in order to integrate external and internal variables. The rules underlying the precise interactions between different prefrontal cortical–subcortical pathways for dynamic social information processing are worthy of future investigation.

The hyperactivity of LHb neurons is linked to social deficits

Our fibre photometry recordings showed that the LHb neurons in naïve mice exhibited only a mild response to social stimuli (Fig. 3). In contrast, in social fear conditioned mice, LHb neurons exhibited highly elevated activity during social fear expression (Fig. 3). In agreement with our study, this phenomenon was also observed during social fear expression induced by social defeat stress.[77] Indeed, direct activation of LHb neurons is sufficient to compromise social interaction behaviour.[58] These lines of evidence strongly suggest that the heightened activity of LHb neurons is linked to social deficits and underlies social fear behaviour when exposed to threatening social stimuli. Although the exact mediators of the LHb in control of social fear behaviour are yet to be determined, the laterodorsal tegmental nucleus and the median raphe region are potential targets. Recent studies have suggested that the laterodorsal tegmental nucleus and the median raphe region, two downstream targets of the LHb, take part in regulating innate and learned fear responses, respectively.[78,79] In addition, given that the LHb directly projects to reward centres, including the VTA and dorsal raphe nucleus,[23] another possibility is that hyperactivity of the mPFC–LHb pathway produces an anti-reward effect. It has been shown that social behaviour and social reward are modulated by VTA dopaminergic projection and dorsal raphe nucleus serotoninergic projection to the nucleus accumbens.[80,81] Hyperactivity of the mPFC–LHb pathway could enhance the inhibitory tone of dopamine neurons and serotonin neurons through local GABAergic interneurons in the VTA and the dorsal raphe nucleus, respectively.[82] Consequently, inhibition of dopaminergic neurons or serotonergic neurons would disrupt social reward processing and eventually

lead to social deficits. In the intact brain, the fear-driving circuits could work in concert with the anti-reward circuits to produce social avoidance behaviour.

The mPFC–LHb pathway as a target for social fear amelioration

In terms of prefrontal–habenular interregional interaction, we found an increased correlation between the activity of LHb-projecting mPFC neurons and that of LHb neurons during social fear expression in mice (Fig. 4). This result is well aligned with a human study showing that the prefrontal cortex and the habenula network exhibited increased synchrony in response to negative emotional stimuli.[83] Anatomically, the mPFC projects to the LHb but not vice versa; therefore, the above findings indicate an excitation of the mPFC–LHb projection by an emotional stimulus with a negative valence, such as during social fear expression. More importantly, we also demonstrated with fMRI that functional connectivity between the prefrontal cortex and the Hb was positively correlated with social anxiety in human subjects (Fig. 6). This observation suggests that an elevated prefrontal–habenular functional connectivity could serve as a potential diagnostic biomarker for social anxiety disorder in subclinical populations. Future research investigating pathological alterations of the functional connectivity between the prefrontal cortex and the Hb in patients with social anxiety disorder should have considerable significance in this regard. Particularly, high spatial resolution fMRI to delineate prefrontal layer-specific functional connectivity with the LHb is warranted to advance our mechanistic understanding of social anxiety disorder in human patients, given our preclinical findings.

In agreement with previous findings,[58] we found that activation of the mPFC–LHb pathway induced social avoidance during social interaction tests (Supplementary Fig. 4). On the contrary, specific inhibition of the mPFC–LHb pathway significantly reduced fear responses in mice with conditioned social fear (Fig. 5). Therefore, social behavioural manifestation is under bidirectional regulation of the mPFC–LHb pathway. Given the close relationship between the hyperactivity of the prefrontal–habenular pathway and social impairments across species, our study is of therapeutic significance. Specifically, taming the hyperactivity of the prefrontal–habenular pathway provides the hope of ameliorating the social fear symptoms often observed in many psychiatric disorders.

Data availability

The data that support the findings of this study will be made available from the corresponding author upon reasonable request.

Acknowledgements

Funding

Competing interests

The authors report no competing interests.

Supplementary material

Supplementary material is available at *Brain* online.

References

1. Maslow AH. A theory of human motivation. *Psychol Rev*. 1943;50: 370-396.
2. Steptoe A, Shankar A, Demakakos P, Wardle J. Social isolation, loneliness, and all-cause mortality in older men and women. *Proc Natl Acad Sci U S A*. 2013;110:5797-5801.
3. Padilla-Coreano N, Tye KM, Zelikowsky M. Dynamic influences on the neural encoding of social valence. *Nat Rev Neurosci*. 2022; 23:535-550.
4. Krishnan V, Han MH, Graham DL, et al. Molecular adaptations underlying susceptibility and resistance to social defeat in brain reward regions. *Cell*. 2007;131:391-404.
5. Li L, Durand-de Cuttoli R, Aubry AV, et al. Social trauma engages lateral septum circuitry to occlude social reward. *Nature*. 2023; 613:696-703.
6. Stein MB, Stein DJ. Social anxiety disorder. *Lancet*. 2008;371: 1115-1125.
7. Leichsenring F, Leweke F. Social anxiety disorder. *N Engl J Med*. 2017;376:2255-2264.
8. Lord C, Elsabbagh M, Baird G, Veenstra-Vanderweele J. Autism spectrum disorder. *Lancet*. 2018;392:508-520.
9. Pallanti S, Quercioli L, Hollander E. Social anxiety in outpatients with schizophrenia: A relevant cause of disability. *Am J Psychiatry*. 2004;161:53-58.
10. Yizhar O, Levy DR. The social dilemma: Prefrontal control of mammalian sociability. *Curr Opin Neurobiol*. 2021;68:67-75.
11. Padilla-Coreano N, Batra K, Patarino M, et al. Cortical ensembles orchestrate social competition through hypothalamic outputs. *Nature*. 2022;603:667-671.
12. Diaz V, Lin D. Neural circuits for coping with social defeat. *Curr Opin Neurobiol*. 2020;60:99-107.
13. Brumback AC, Ellwood IT, Kjaerby C, et al. Identifying specific prefrontal neurons that contribute to autism-associated abnormalities in physiology and social behavior. *Mol Psychiatry*. 2018; 23:2078-2089.
14. Zhao Z, Zeng F, Wang H, et al. Encoding of social novelty by sparse GABAergic neural ensembles in the prelimbic cortex. *Sci Adv*. 2022;8:eabo4884.
15. Bruhl AB, Delsignore A, Komossa K, Weidt S. Neuroimaging in social anxiety disorder—A meta-analytic review resulting in a new neurofunctional model. *Neurosci Biobehav Rev*. 2014;47: 260-280.
16. Numa C, Nagai H, Taniguchi M, Nagai M, Shinohara R, Furuyashiki T. Social defeat stress-specific increase in c-Fos expression in the extended amygdala in mice: Involvement of dopamine D1 receptor in the medial prefrontal cortex. *Sci Rep*. 2019;9:16670.

17. Xu H, Liu L, Tian Y, et al. A disinhibitory microcircuit mediates conditioned social fear in the prefrontal cortex. *Neuron*. 2019; 102:668-682.e5.

18. Hare BD, Duman RS. Prefrontal cortex circuits in depression and anxiety: Contribution of discrete neuronal populations and target regions. *Mol Psychiatry*. 2020;25:2742-2758.

19. Huang W-C, Zucca A, Levy J, Page DT. Social behavior is modulated by valence-encoding mPFC-amygdala sub-circuitry. *Cell Rep*. 2020;32:107899.

20. Murugan M, Jang HJ, Park M, et al. Combined social and spatial coding in a descending projection from the prefrontal cortex. *Cell*. 2017;171:1663-1677.e16.

21. Park G, Ryu C, Kim S, et al. Social isolation impairs the prefrontal-nucleus accumbens circuit subserving social recognition in mice. *Cell Rep*. 2021;35:109104.

22. Yamamuro K, Bicks LK, Leventhal MB, et al. A prefrontal–paraventricular thalamus circuit requires juvenile social experience to regulate adult sociability in mice. *Nat Neurosci*. 2020;23: 1240-1252.

23. Hu H, Cui Y, Yang Y. Circuits and functions of the lateral habenula in health and in disease. *Nat Rev Neurosci*. 2020;21:277-295.

24. Kim U, Lee T. Topography of descending projections from anterior insular and medial prefrontal regions to the lateral habenula of the epithalamus in the rat. *Eur J Neurosci*. 2012;35:1253-1269.

25. Hashikawa Y, Hashikawa K, Rossi MA, et al. Transcriptional and spatial resolution of cell types in the mammalian habenula. *Neuron*. 2020;106:743-758.e5.

26. Huang L, Xi Y, Peng Y, et al. A visual circuit related to habenula underlies the antidepressive effects of light therapy. *Neuron*. 2019;102:128-142.e8.

27. Yang Y, Cui Y, Sang K, et al. Ketamine blocks bursting in the lateral habenula to rapidly relieve depression. *Nature*. 2018;554: 317-322.

28. Fan Z, Chang J, Liang Y, et al. Neural mechanism underlying depressive-like state associated with social status loss. *Cell*. 2023;186:560-576.e17.

29. Sachs BD, Ni JR, Caron MG. Brain 5-HT deficiency increases stress vulnerability and impairs antidepressant responses following psychosocial stress. *Proc Natl Acad Sci U S A*. 2015;112: 2557-2562.

30. Lecca S, Namboodiri VMK, Restivo L, et al. Heterogeneous habenular neuronal ensembles during selection of defensive behaviors. *Cell Rep*. 2020;31:107752.

31. Toth I, Neumann ID, Slattery DA. Social fear conditioning: A novel and specific animal model to study social anxiety disorder. *Neuropsychopharmacology*. 2012;37:1433-1443.

32. Zoicas I, Slattery DA, Neumann ID. Brain oxytocin in social fear conditioning and its extinction: Involvement of the lateral septum. *Neuropsychopharmacology*. 2014;39:3027-3035.

33. Zheng J, Tian Y, Xu H, Gu L, Xu H. A standardized protocol for the induction of specific social fear in mice. *Neurosci Bull*. 2021;37: 1708-1712.

34. Tsien JZ, Chen DF, Gerber D, et al. Subregion- and cell type-restricted gene knockout in mouse brain. *Cell*. 1996;87: 1317-1326.

35. Golden SA, Covington HE III, Berton O, Russo SJ. A standardized protocol for repeated social defeat stress in mice. *Nat Protoc*. 2011;6:1183-1191.

36. Franklin TB, Silva BA, Perova Z, et al. Prefrontal cortical control of a brainstem social behavior circuit. *Nat Neurosci*. 2017;20: 260-270.

37. Golden SA, Heshmati M, Flanigan M, et al. Basal forebrain projections to the lateral habenula modulate aggression reward. *Nature*. 2016;534:688-692.

38. Chaudhury D, Walsh JJ, Friedman AK, et al. Rapid regulation of depression-related behaviours by control of midbrain dopamine neurons. *Nature*. 2013;493:532-536.

39. He Z, Young L, Ma XM, et al. Increased anxiety and decreased sociability induced by paternal deprivation involve the PVN-PrL OTergic pathway. *Elife*. 2019;8:e44026.

40. Wang Y, You L, Tan K, et al. A common thalamic hub for general and defensive arousal control. *Neuron*. 2023;111:3270-3287.e8.

41. Wei J-A, Han Q, Luo Z, et al. Amygdala neural ensemble mediates mouse social investigation behaviors. *Natl Sci Rev*. 2023; 10:nwac179.

42. Guo B, Chen J, Chen Q, et al. Anterior cingulate cortex dysfunction underlies social deficits in *Shank3* mutant mice. *Nat Neurosci*. 2019;22:1223-1234.

43. Liebowitz MR. Social phobia. *Mod Probl Pharmacopsychiatry*. 1987; 22:141-173.

44. He Y, Zhang M. Psychometric investigation of Liebowitz social anxiety scale. *J Diagn Concepts Pract*. 2004;3:89-93.

45. Oakman J, Van Ameringen M, Mancini C, Farvolden P. A confirmatory factor analysis of a self-report version of the Liebowitz social anxiety scale. *J Clin Psychol*. 2003;59:149-161.

46. Heimberg RG, Horner KJ, Juster HR, et al. Psychometric properties of the Liebowitz social anxiety scale. *Psychol Med*. 1999;29: 199-212.

47. Derogatis LR, Savitz KL. The SCL-90-R, Brief Symptom Inventory, and Matching Clinical Rating Scales. In: Maruish ME, ed. *The use of psychological testing for treatment planning and outcomes assessment*. 2nd edn. Lawrence Erlbaum Associates; 1999:679-724.

48. Avants B, Tustison N, Song G. Advanced normalization tools (ANTS). *Insight J*. 2009;2:1-35.

49. Cox RW. AFNI: Software for analysis and visualization of functional magnetic resonance neuroimages. *J Comput Biomed Res*. 1996;29:162-173.

50. D'Ardenne K, McClure SM, Nystrom LE, Cohen JD. BOLD responses reflecting dopaminergic signals in the human ventral tegmental area. *Science*. 2008;319:1264-1267.

51. Lawson RP, Drevets WC, Roiser JP. Defining the habenula in human neuroimaging studies. *Neuroimage*. 2013;64:722-727.

52. Yarkoni T, Poldrack RA, Nichols TE, Van Essen DC, Wager TD. Large-scale automated synthesis of human functional neuroimaging data. *Nat Methods*. 2011;8:665-670.

53. Keith BJ, Franklin GP. *The mouse brain in stereotaxic coordinates*, 3rd edn. Academic Press; 2007.

54. Liu XB, Jones EG. Localization of alpha type II calcium calmodulin-dependent protein kinase at glutamatergic but not gamma-aminobutyric acid (GABAergic) synapses in thalamus and cerebral cortex. *Proc Natl Acad Sci U S A*. 1996;93:7332-7336.

55. Warden MR, Selimbeyoglu A, Mirzabekov JJ, et al. A prefrontal cortex-brainstem neuronal projection that controls response to behavioural challenge. *Nature*. 2012;492:428-432.

56. Liu WZ, Zhang WH, Zheng ZH, et al. Identification of a prefrontal cortex-to-amygdala pathway for chronic stress-induced anxiety. *Nat Commun*. 2020;11:2221.

57. Han S-W, Kim Y-C, Narayanan NS. Projection targets of medial frontal D1DR-expressing neurons. *Neurosci Lett*. 2017;655:166-171.

58. Benekareddy M, Stachniak TJ, Bruns A, et al. Identification of a corticohabenular circuit regulating socially directed behavior. *Biol Psychiatry*. 2018;83:607-617.

59. Zhang W, Feng C, Zhang Y, Guan Q, Luo Y, Yang S. The effects of aversive mood state on the affective anticipation and perception: An event-related potential study. *Neuroscience*. 2021;458:133-140.

60. Calhoon GG, Tye KM. Resolving the neural circuits of anxiety. *Nat Neurosci*. 2015;18:1394-1404.

61. Ely BA, Stern ER, Kim JW, Gabbay V, Xu J. Detailed mapping of human habenula resting-state functional connectivity. *Neuroimage*. 2019;200:621-634.

62. Anastasiades PG, Carter AG. Circuit organization of the rodent medial prefrontal cortex. *Trends Neurosci*. 2021;44:550-563.

63. Gabbott PLA, Warner TA, Jays PRL, Salway P, Busby SJ. Prefrontal cortex in the rat: Projections to subcortical autonomic, motor, and limbic centers. *J Comp Neurol*. 2005;492:145-177.

64. Tovote P, Fadok JP, Luthi A. Neuronal circuits for fear and anxiety. *Nat Rev Neurosci*. 2015;16:317-331.

65. de Kloet SF, Bruinsma B, Terra H, et al. Bi-directional regulation of cognitive control by distinct prefrontal cortical output neurons to thalamus and striatum. *Nat Commun*. 1994;12:1994.

66. Otis JM, Namboodiri VM, Matan AM, et al. Prefrontal cortex output circuits guide reward seeking through divergent cue encoding. *Nature*. 2017;543:103-107.

67. Burgos-Robles A, Vidal-Gonzalez I, Quirk GJ. Sustained conditioned responses in prelimbic prefrontal neurons are correlated with fear expression and extinction failure. *J Neurosci*. 2009;29:8474-8482.

68. Silva BA, Gross CT, Graff J. The neural circuits of innate fear: Detection, integration, action, and memorization. *Learn Mem*. 2016;23:544-555.

69. Courtin J, Chaudun F, Rozeske RR, et al. Prefrontal parvalbumin interneurons shape neuronal activity to drive fear expression. *Nature*. 2014;505:92-96.

70. Cummings KA, Clem RL. Prefrontal somatostatin interneurons encode fear memory. *Nat Neurosci*. 2020;23:61-74.

71. Do-Monte FH, Quinones-Laracuente K, Quirk GJ. A temporal shift in the circuits mediating retrieval of fear memory. *Nature*. 2015;519:460-463.

72. Rozeske RR, Jercog D, Karalis N, et al. Prefrontal-periaqueductal gray-projecting neurons mediate context fear discrimination. *Neuron*. 2018;97:898-910.e6.

73. Noh YW, Kim Y, Lee S, et al. The PFC-LH-VTA pathway contributes to social deficits in IRSp53-mutant mice. *Mol Psychiatry*. 2023;28:4642-4654.

74. Menon R, Neumann ID. Detection, processing and reinforcement of social cues: Regulation by the oxytocin system. *Nat Rev Neurosci*. 2023;24:761-777.

75. Yu H, Miao W, Ji E, et al. Social touch-like tactile stimulation activates a tachykinin 1-oxytocin pathway to promote social interactions. *Neuron*. 2022;110:1051-1067.e7.

76. Froemke RC, Young LJ. Oxytocin, neural plasticity, and social behavior. *Annu Rev Neurosci*. 2021;44:359-381.

77. Wang D, Li Y, Feng Q, Guo Q, Zhou J, Luo M. Learning shapes the aversion and reward responses of lateral habenula neurons. *Elife*. 2017;6:e23045.

78. Yang H, Yang J, Xi W, et al. Laterodorsal tegmentum interneuron subtypes oppositely regulate olfactory cue-induced innate fear. *Nat Neurosci*. 2016;19:283-289.

79. Szonyi A, Zicho K, Barth AM, et al. Median raphe controls acquisition of negative experience in the mouse. *Science*. 2019;366:eaay8746.

80. Hung LW, Neuner S, Polepalli JS, et al. Gating of social reward by oxytocin in the ventral tegmental area. *Science*. 2017;357:1406-1411.

81. Dolen G, Darvishzadeh A, Huang KW, Malenka RC. Social reward requires coordinated activity of nucleus accumbens oxytocin and serotonin. *Nature*. 2013;501:179-184.

82. Proulx CD, Hikosaka O, Malinow R. Reward processing by the lateral habenula in normal and depressive behaviors. *Nat Neurosci*. 2014;17:1146-1152.

83. Huang Y, Sun B, Debarros J, et al. Increased theta/alpha synchrony in the habenula-prefrontal network with negative emotional stimuli in human patients. *Elife*. 2021;10:e65444.